buildings

MDPI

Article

Fatigue Life Prediction for Stud Shear Connectors Based on a Machine Learning Model

Dong-Hyun Kang [1], Gi-Tae Roh [1], Chang-Su Shim [1,*] and Kyoung-Chan Lee [2]

[1] Department of Civil and Environmental Engineering, Chung-Ang University, Seoul 06974, Republic of Korea; rkdehdgus@cau.ac.kr (D.-H.K.); shrlxo2001@cau.ac.kr (G.-T.R.)
[2] Department of Civil and Railroad Engineering, Pai Chai University, Daejeon 35345, Republic of Korea; kclee@pcu.ac.kr
* Correspondence: csshim@cau.ac.kr

Abstract: The shear connector of a steel composite bridge is designed by predicting fatigue life using the fatigue strength curves (S-N curve) based on push-out test results. The fatigue strength curves of the current design codes present only a linear relationship between the stress range and fatigue life on a log scale based on push-out experiment results. However, an alternative to the current empirical formula is necessary for the fatigue design of shear connections involving many detailed variations or high strength steel materials. This study collected and reanalyzed data from push-out fatigue tests to determine the factors influencing fatigue life and propose a machine learning-based fatigue life prediction model. The proposed machine learning model demonstrated an improvement in predictive performance of approximately 2 to 8 times compared to the existing design codes when evaluated against experimental data. Feature importance analysis based on the proposed model revealed that the stress range most significantly influenced fatigue life prediction. Model validation results indicated that the proposed model provided reliable predictions with accuracy and generalization performance. Moreover, it effectively accounted for uncertainty by incorporating features previously overlooked in existing design codes. Plans for fine-tuning pretrained models were also discussed.

Keywords: machine learning; stud shear connection; fatigue life prediction; composite bridge; gaussian process regression; pretrained model

check for updates

Citation: Kang, D.-H.; Roh, G.-T.; Shim, C.-S.; Lee, K.-C. Fatigue Life Prediction for Stud Shear Connectors Based on a Machine Learning Model. *Buildings* **2024**, *14*, 3278. https://doi.org/10.3390/buildings14103278

Academic Editor: Hiroshi Tagawa

Received: 13 September 2024
Revised: 9 October 2024
Accepted: 15 October 2024
Published: 16 October 2024

Copyright: © 2024 by the authors. Licensee MDPI, Basel, Switzerland. This article is an open access article distributed under the terms and conditions of the Creative Commons Attribution (CC BY) license (https://creativecommons.org/licenses/by/4.0/).

1. Introduction

Welded stud shear connectors are critical components in the design of a steel concrete composite bridge, demonstrating reliable performance for over 60 years. These connectors are typically installed using welding guns. The fatigue life of the stud connectors primarily governs the design of shear connections in composite bridges. However, current design codes are based on a relatively limited dataset, often involving standard details. For example, the AASHTO LRFD Bridge Design Specifications were derived from only 44 push-out tests [1]. According to the AASHTO [2], the fatigue shear resistance of an individual stud shear connector, Z_r, is given by Equation (1). Notably, the fatigue life of stud shear connectors is predominantly influenced by their stress ranges.

$$Z_r = \alpha d^2 \geq \frac{38.0}{2} d^2 \quad (1)$$

where $\alpha = 238 - 29.5 \log N$; d = stud diameter (mm), and N = number of fatigue cycles.

Oehlers and Foley [3] developed a peak load model that considers the maximum shear force, P_p, based on 280 push tests. However, as Johnson [4] highlighted, discrepancies in fatigue life predictions among different researchers are primarily attributed to the scatter in the test data and differences in the regression analyses. These inconsistencies underscore

the challenges in achieving a consensus on fatigue life prediction. In addition, Eurocode 4 [5] provisions for the fatigue of stud shear connectors are constrained by limitations in the underlying design parameters, influenced by the specific set of background data used in their development. The magnitude of the peak load, P_{max}, of the cyclic loading exhibited a significant effect. Consequently, Hanswille et al. [6,7] proposed a modified damage accumulation hypothesis.

$$N_f \left(\frac{\Delta P}{P_R} \right)^m = 10^k \quad (2)$$

ΔP is the range of shear force;
P_R is the static shear strength of the stud;
$N_f = N_e / \left[1 - \left(\frac{P_p}{P_R} \right) \right]$;
N_e is the endurance of uni-directionally loaded specimen;
P_p is peak shear force per stud;
k is characteristic (2.3% fractile for a normal distribution).

Variations in stud shear connection practices primarily include the use of large-diameter studs [8,9], high-performance concrete [10], specific details of shear pockets in precast decks [11], and the group arrangement of studs [12–14]. These variations are illustrated in Figure 1. These design variables, falling outside the scope of current design codes, significantly impact static strength and fatigue life predictions. The diversity of materials and configurations used in stud shear connections for steel concrete composite bridges poses challenges for effectively applying existing design codes in practice.

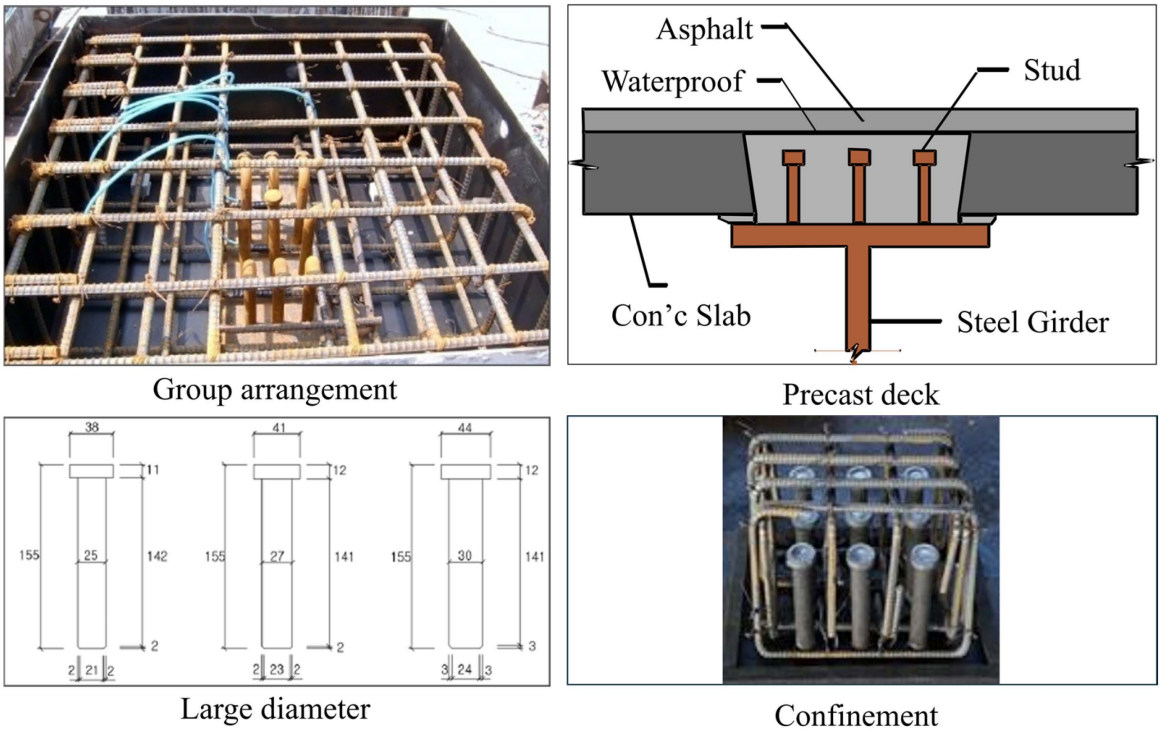


Figure 1. Variation in stud shear connector [12].

Current design criteria for evaluating fatigue life primarily rely on empirical formulas derived from previous experimental data. These formulas are largely based on tests using 19 and 22 mm diameters stud connectors, often with varying experimental setups, including single and double-sided configurations [15]. Although this empirical approach provides a conservative estimate of stud fatigue life, it does not account for critical factors such as the effects of maximum stress, influence of mortar fillers without high-strength concrete or

coarse aggregate, and impact of constraints. Consequently, current criteria may not fully capture the complexities of modern materials and design conditions.

To address the limitations of existing design codes, some researchers have explored the replacement of conventional empirical formulas with machine learning models. Using a data-driven approach, machine learning models can overcome challenges, such as limited data availability, uncertainty quantification, and the evaluation and consideration of various influencing not included in current design codes. Avci-Karatas [16] developed advanced machine learning models to predict the shear capacity of headed shear studs using minimax probability machine regression (MPMR) and extreme machine learning (EML). These models were compared and validated against the static strength equations of existing design codes. Rho et al. [17] proposed a machine learning model that integrates finite element method data with experimental data. They introduced the concept of a digital twin model for the static design of stud shear connectors with push-out specimens to replace empirical design codes. Roshanfar et al. [18] compared the performance of six machine learning models in predicting the fatigue life of shear connectors and compared the results with current design codes (Table 1).

Table 1. Research on the replacement of design codes using machine learning.

Reference	Objective	Data and Features	Methodology
Avci-Karatas [16]	Shear capacity of headed stud	Number of data: 215	Minimax probability machine regression (MPMR)
		Features: D, f_{cm}, f_u	Extreme Machine Learning (EML)
Roh et al. [17]	Shear capacity of headed stud	Number of data (Strength): 431 Number of data (Slip): 194	Catboost Xgboost Random forest LightGBM ExtraTrees
		Features: Dimension for stud (D_{sc}, h_{sc}), Confinements (confinement ratio, diameter, f_y) slab (b (mm), d (mm), t (mm)), Concrete material (E_{cm}, f_{cm}) Steel material (E_s, f_u)	
Roshanfar et al. [18]	Fatigue life of shear connector	Number of data:	Linear regression
		Features: Shear stress range of shear connector Compressive strength, Shear strength of shear connector Diameter Type of test Type of shear connector	Decision tree
			Support vector Regressor
			Gaussian process regression (GPR) Bagged tree (BT) Artificial neural network

Machine learning models heavily rely on analyzing the relationship between input and output data using algorithms that maximize outcomes. However, this approach is highly dependent on data quality, posing substantial challenges, particularly when experimental data are limited. In cases where data availability is constrained, such as in regression analysis or artificial intelligence (AI)-based models, reliance on conventional models can lead to difficulties in inferring clear causal relationships. This may reduce the reliability of outcomes and lead to issues such as overfitting.

To address these challenges, an increasing demand for explainable AI models has emerged, gaining widespread applications across various fields. These models validate outcomes by comparing input and output values, and investigating variable correlations through rational processes (e.g., SHapley Addictive exPlanations (SHAP)). In addition, they incorporate methods such as physics-informed machine learning, which replaces the data required for conventional training with physics-based equations (e.g., differential equations) commonly used in engineering fields.

This study proposes a machine learning-based model for predicting the fatigue life of stud shear connectors, as illustrated in Figure 2. To enhance the model performance, we performed feature engineering by analyzing the correlations and causal relationships among the factors influencing fatigue behavior, as identified in previous research. Subsequently, we eliminated features that impaired accuracy owing to linear interdependence among input data and fatigue life with high sensitivity for training. To derive the model outcomes, we further analyzed the significance and trends of the selected variables within the model through feature importance analysis using individual conditional expectation (ICE) and SHAP. Ultimately, this study proposes a pretrained machine learning model, trained on global data from referenced literature, as an alternative to the existing design codes. In addition, it presents the foundation for a fine-tuning model that can be further trained with local data in future.

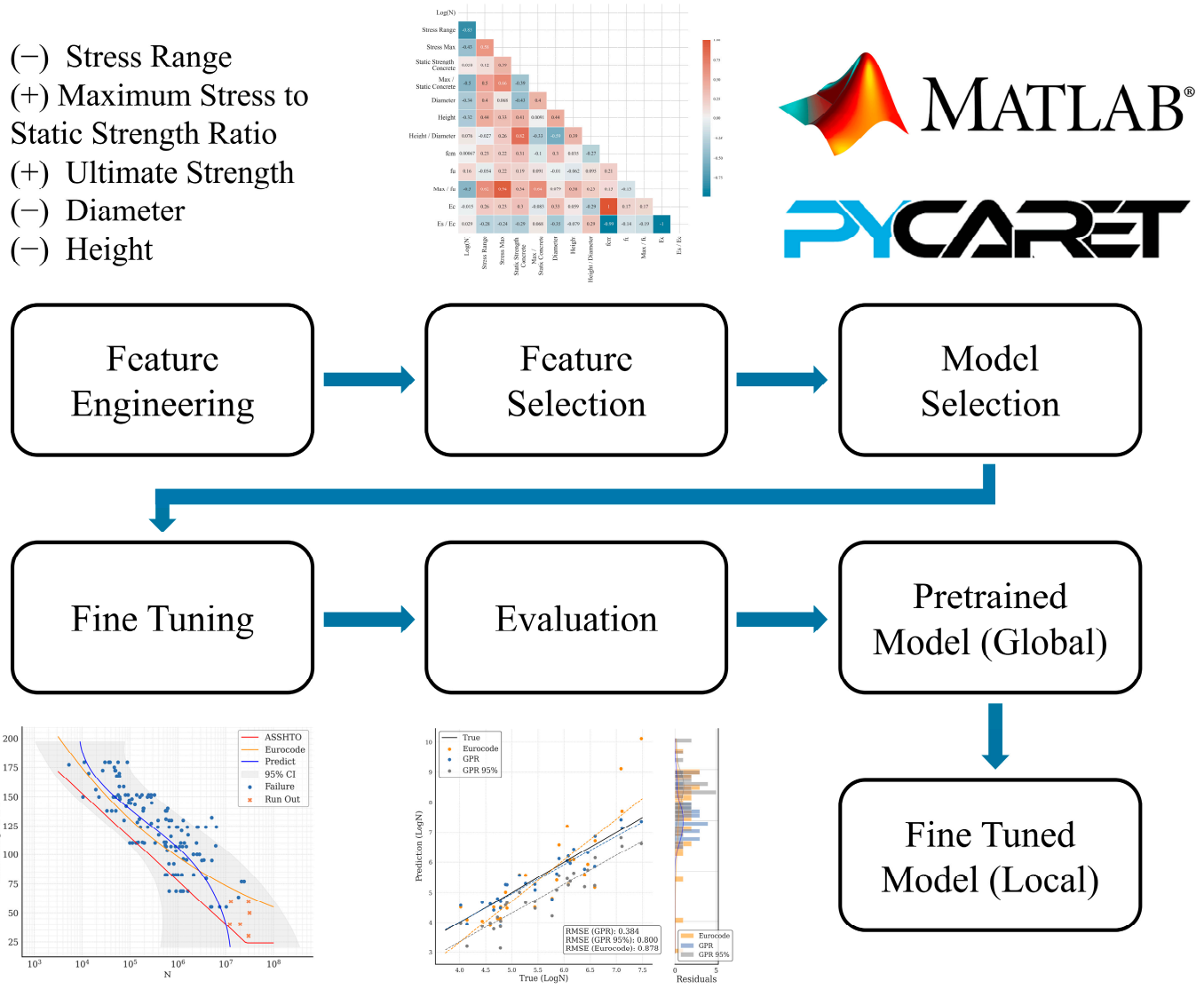


Figure 2. Fatigue life prediction based on a machine learning model.

2. Dataset

2.1. Data Preprocessing

Push-out test data collected from 1966 to 2016 were analyzed to predict the fatigue life of shear connectors. Through feature engineering, factors affect to fatigue life were identified, and relevant physical features were selected. Subsequently, feature selection

was conducted to analyze the linearity and select the most reasonable features. Ultimately, a dataset for predicting fatigue life was developed.

2.2. Feature Engineering

To determine the features affecting fatigue behavior and analyze causality, fatigue behavior was categorized into shear transfer under fatigue loading, crack initiation, crack propagation, and fatigue failure.

2.2.1. Mechanism of Shear Transfer by Dowel Action

Figure 3 illustrates the mechanism of shear transfer by dowel action when a cyclic load is applied to a push-out specimen. Under cyclic load, the resultant force, F, in the bearing zone occurs with eccentricity, e, and induces high tensile stresses in the steel failure zone. Oehler and Bradford [19] stated that "in the concrete adjacent to the bearing zone has to withstand compressive stresses of about seven times the cylinder strength of the concrete f_c, and this can only be achieved by the triaxial restraint imposed on the region by the streel element, the dowel and the surrounding concrete".

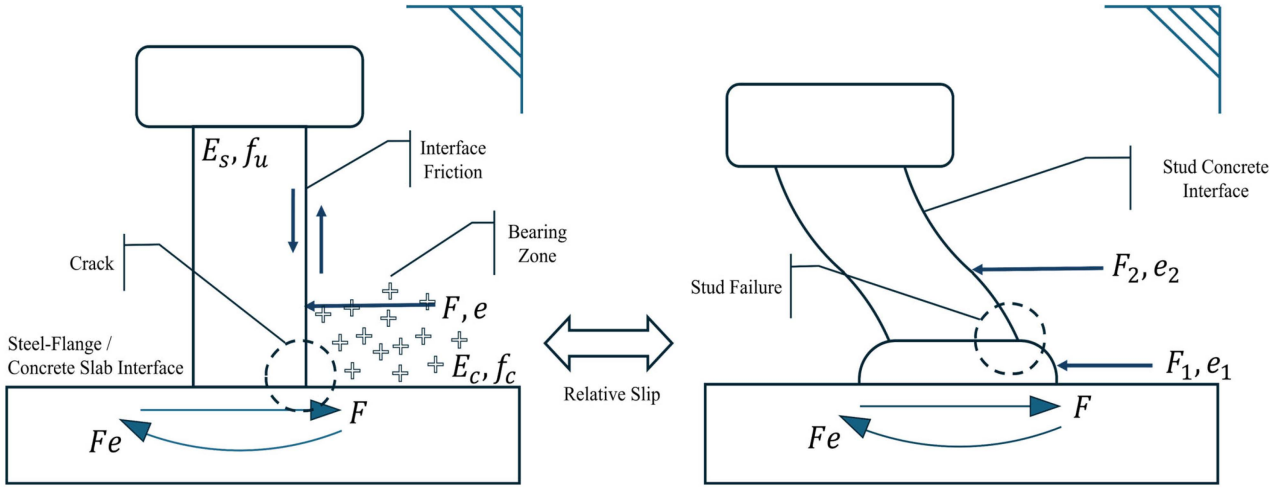


Figure 3. Idealized model of shear transfer by dowel action.

The stress range and maximum stress on the shear connectors induced by cyclic loading, compressive strength of the concrete in the bearing zone, and ultimate strength of the stud were identified as the key features influencing fatigue life in shear transfer.

2.2.2. Crack Initiation

Cracks in welded shear studs typically initiate at the welded part. In smooth-surfaced parts subjected to cyclic loading, dislocation and deformations of crystallographic planes result in surface roughening. Consequently, numerous micro-cracks form along the slip planes. Continued cyclic loading causes some of these micro-cracks to merge and form dominant cracks. The stress at the tips of these larger cracks is extremely high, causing them to propagate more rapidly [20].

Therefore, the peak load of the cyclic load and welding specifications and quality were determined as factors influencing crack initiation. However, for the welding quality, which cannot be quantified, Lee et al. [9] stated that "As the large stud has a lager cross-sectional area, welding required a power source with higher amperage. It affects to the lower of fatigue life in push out test which lead to an unfavorable welding collar". Thus, stud diameter was also identified as an influencing feature indirectly reflecting the effect of welding quality on crack initiation.

2.2.3. Crack Propagation

During cyclic loading, the crack propagation rate in the steel failure zone of the stud is proportional to the stress intensity factor K according to Paris's power law [21]. This factor is a function of the stress at the crack tip, which is proportional to the energy release rate, G. Based on this relationship, the behavior of the stud can be distinguished into cantilever behavior and steel beam supported by an elastic concrete medium [19].

If the stud behaves as a cantilever under cyclic loading, the uncracked area decreases as the crack propagates. This reduction in the uncracked area increases the stress at the crack tip. This increases the energy release rate, accelerating crack propagation. Conversely, if the stud acts as a steel beam supported by an elastic concrete medium, the concrete resists the cyclic load, reducing the eccentricity. This reduces the stress at the crack tip. Consequently, the energy release rate decreases, leading to a reduced crack propagation rate. However, in actual behavior, reduced eccentricity, reduces the area of concrete resisting the load also decreases. This increases the stress on the concrete, causing concrete crushing and affecting the energy release rate. In addition, friction at the stud prevents the crack tip from opening and reduces the stress at the crack tip.

In existing design codes, fatigue life is defined under the assumption that the ultimate and fatigue limit states are independent. However, in push-out tests, fatigue life is typically determined based on the number of cycles at which significant deformation is observed; therefore, the assumption that static strength is preserved until cyclic loading is not desirable. Consequently, researchers have explained that the repeated loading reduces static strength of shear studs [3,6]. Based on this assumption, Hanswille et al. [6,7] performed 71 push-out tests to determine the reduction in static strength after cyclic loading and proposed a fatigue life model that considers the ratio between the peak load and static strength.

Therefore, during the crack propagation process, the stress range, maximum stress under peak load, concrete compressive strength, stud height for reflecting friction, static strength, and their ratio between peak load and static strength derived from existing experiments and analyses were selected as the influencing features.

2.2.4. Failure

As the crack propagates, the dowel shear mechanism can be represented by an interaction model of an equivalent steel beam and concrete subjected to force, F, with eccentricity, e. In this model, an increase in the ratio of the elastic modulus of the steel beam to that of the concrete, $\frac{E_s}{E_c}$, results in greater eccentricity, reducing the dowel strength.

In addition, if the concrete is crushed during crack propagation, its elastic modulus, E_c, decreases, increasing eccentricity. This increases the flexural stress in the steel failure zone, accelerating crack propagation. Consequently, increasing $\frac{E_s}{E_c}$ further increases eccentricity and the bearing pressure on the concrete, causing concrete crushing. This process repeats, ultimately leading to failure. Therefore, to account for the interaction between the stud and concrete after crack propagation leading to failure, the ratio of the elastic modulus of the stud to that of the concrete was selected as a feature.

2.2.5. Feature Definition

The analysis of the fatigue behavior of shear connections and the factors influencing fatigue life, along with the relationships between each feature, is illustrated in the fishbone diagram in Figure 4.

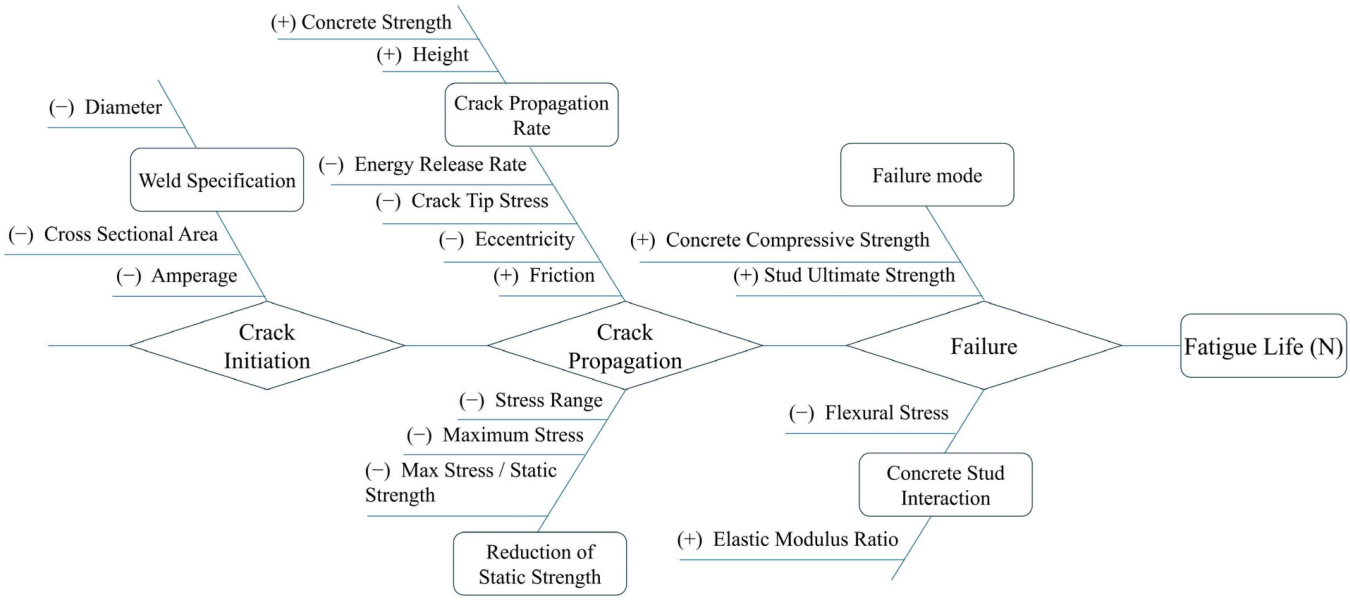


Figure 4. Causality diagram for fatigue life prediction.

The features influencing fatigue life are defined as follows: The N value, representing fatigue life, refers to the number of load cycles at which failure or significant displacement occurs. However, for run-out data in which failure did not occur, the last observed number of cycles is designated as the fatigue life. The stress range and maximum stress values are defined as the stress per stud during cyclic loading. The compressive strength of concrete is determined by the mean cylindrical compressive strength of concrete in the bearing zone, where interaction with the studs occurs. The average value from the direct compressive strength test is used. If compressive strength tests are not performed and an f_{ck} value is provided, it is converted to f_{cm} using Equation (3) from the Eurocode.

$$f_{cm} = f_{ck} + 8 \quad (\text{MPa}) \tag{3}$$

$$f_{cylinder} = 0.85 f_{cube} \tag{4}$$

In cases where the $f_{ck,cube}$ value of cubic specimens is provided, it is converted to the cylinder value, f_{ck}, according to the relevant code, and then reflected as f_{cm}. Because most experiments do not specify the elastic modulus of concrete, it is calculated using Equation (5) from the Eurocode. For static strength, the material properties from each test are converted using Equation (6) from the Eurocode.

$$E_{cm} = 22,000 * \left[\frac{f_{cm}}{10}\right]^{0.3} \quad (\text{MPa}) \tag{5}$$

If the test program does not include a static strength experiment, the static strength equation from Equation (6), according to Eurocode 4 [5], is adopted to reflect each failure mode.

$$P_{Rd} = \min\left(\frac{0.29\alpha d_s^2\sqrt{f_{ck}E_c}}{r_v}, \frac{0.8 f_u\left(\frac{\pi d_s^2}{4}\right)}{r_v}\right), \text{ where } r_v = 1.25$$
$$\left(\alpha = 0.2\left(\frac{h_{sc}}{d} + 1\right) for\ 3 \le \frac{h_{sc}}{d} \le 4\right) \tag{6}$$

To account for concrete crushing, the static strength by the combined damage from bearing concrete and stud connector, $Q_{u,\,concrete}$, and its ratio to the maximum stress, $\sigma_{max}/Q_{u,\,concrete}$, are selected as features. In addition, to reflect the ultimate failure mode of

the stud, the ultimate strength of the stud f_u and its ratio with the maximum stress σ_{max}/f_u are selected as features (Table 2).

$$Q_{u,concrete} = 0.29\alpha d_s^2\sqrt{f_{ck}E_c}, \text{ where } \alpha = 0.2\left(\frac{h_{sc}}{d}+1\right) \quad (7)$$

Table 2. Features for fatigue life prediction by the feature engineering.

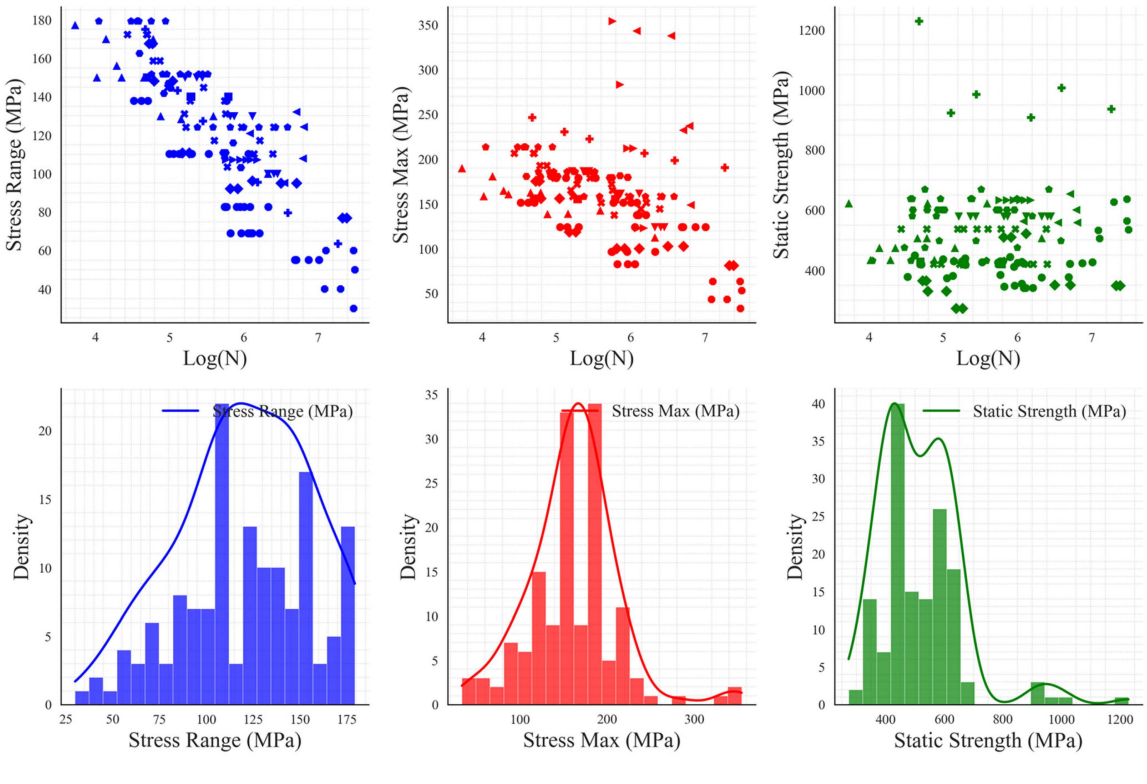
Name	Symbol	Definition	Unit
Stress range	σ_{range}	Range of stress per stud under cyclic load	mm
Stress max	σ_{max}	Stress per stud under peak load	MPa
Concrete static strength	$Q_{u,\ concrete}$	Static Strength by local concrete pressure according to Eurocode 4	MPa
Maximum stress concrete ratio	$\sigma_{max}/Q_{u,concete}$	Ratio of maximum stress to static strength by local concrete pressure	None
Diameter	d	Nominal diameter of shear stud	MPa
Height	h	Height of shear stud	MPa
Height diameter ratio	h/d	Height to diameter ratio of shear stud	None
Concrete compressive strength	f_{cm}	Mean value of concrete cylinder compressive strength	MPa
Ultimate strength	f_u	Ultimate strength of shear stud	MPa
Maximum stress ultimate ratio	σ_{max}/f_u	Ratio of maximum stress to ultimate strength of shear stud	None
Concrete elastic modulus	E_c	Concrete elastic modulus from f_{cm} according to Eurocode 2	MPa
Elastic modulus ratio	$\frac{E_s}{E_c}$	Ratio of stud elastic modulus (assumed as 200,000 MPa) to Concrete Elastic Modulus	None
Name	**Symbol**	**Definition**	**Unit**
LogN	N	Log scale cycles	Cycle

2.3. Feature Selection

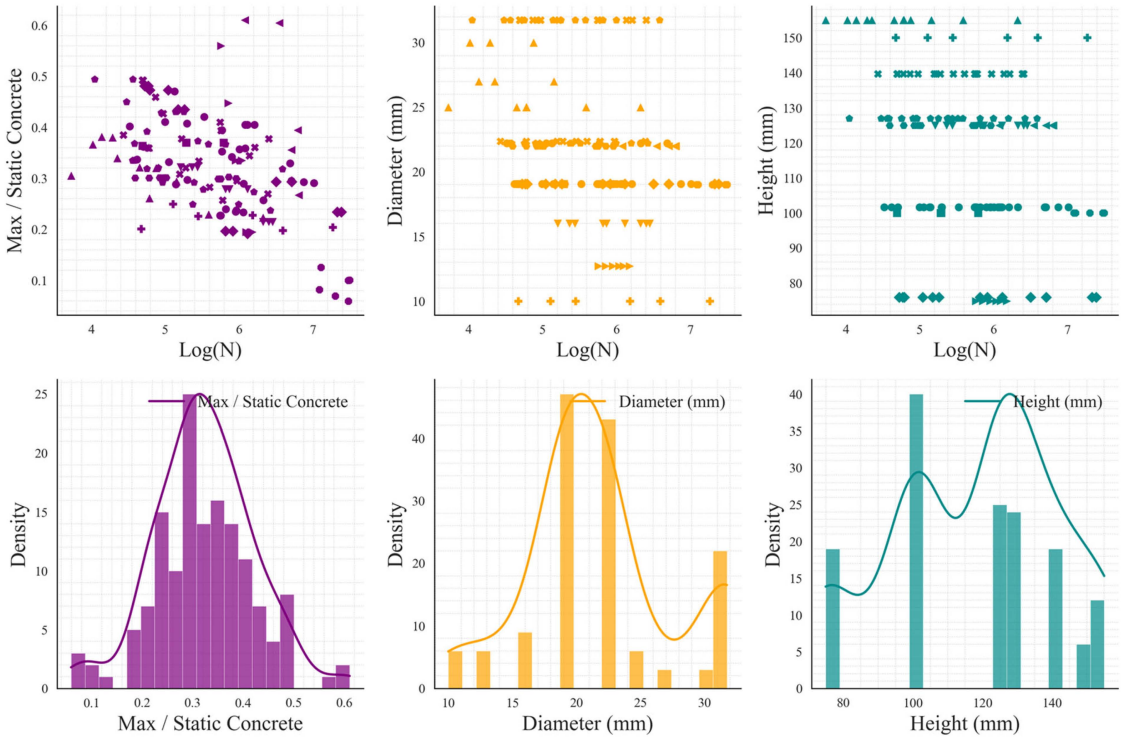
Among the previously identified features, the final selection of features for constructing the dataset for stud fatigue life prediction was made through data filtering, which involved identifying and removing data that could hinder model training. In addition, a correlation coefficient matrix was analyzed to assess the relationships between the features.

2.3.1. Data Filtering

During the filtering of the collected data, some experiments were identified as outliers that negatively impacted the performance of the machine learning model and were excluded from the dataset. For example, the experiments performed by Mainstone and Menzies [22] were excluded because they significantly underestimated fatigue life. This underestimation was attributed to the high maximum stress ratio ranging from 0.6 to 0.87. This leads to earlier concrete crushing with a lack of reinforcement, resulting in insufficient geometric constraints. Consequently, 145 records [1,6,9,20,22–31] were selected as the final dataset for fatigue life prediction, Figure 5 shows scatter plots and histograms of each feature.



(**a**)



(**b**)

Figure 5. *Cont.*

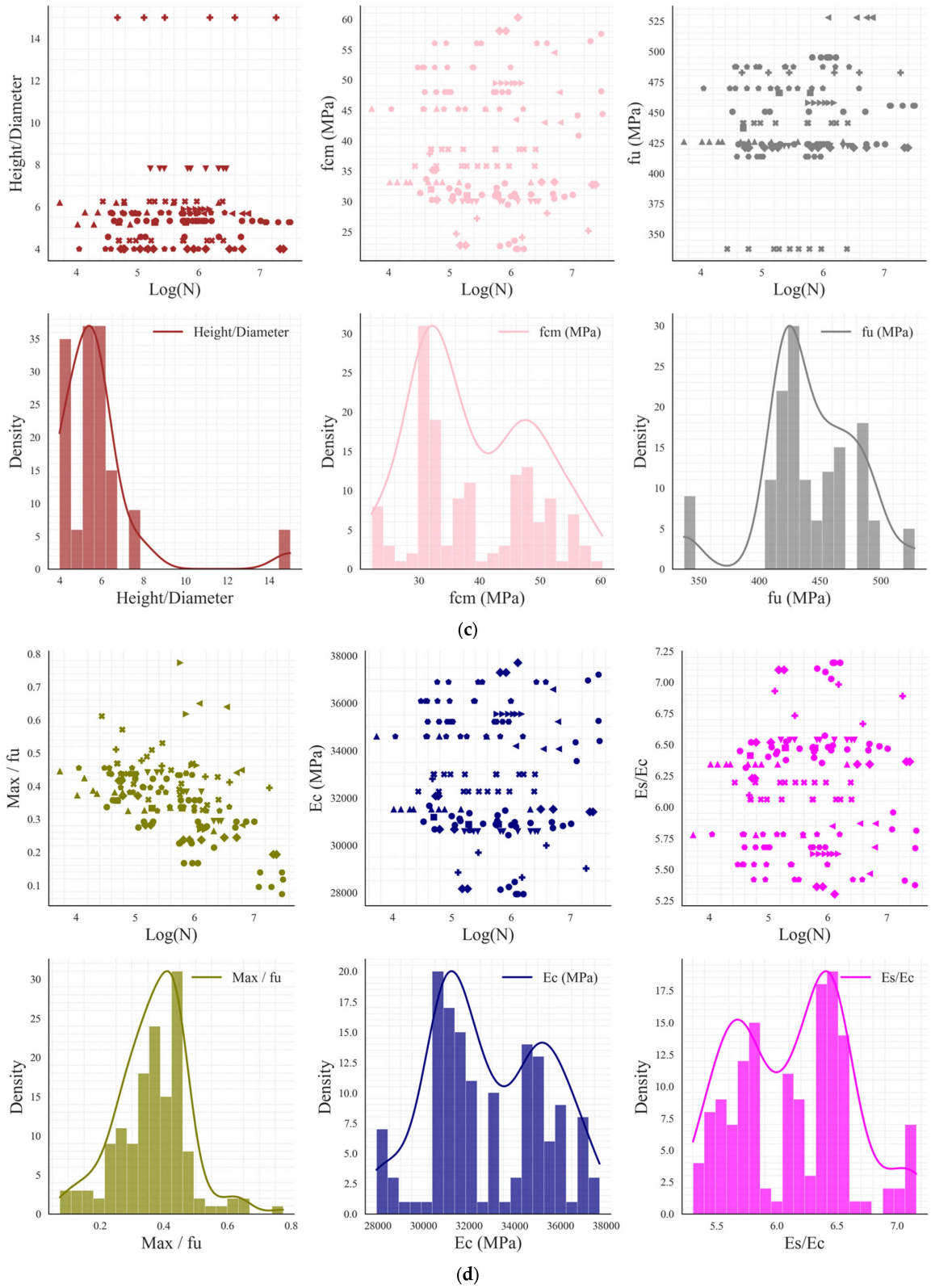


Figure 5. Scatter plot and histogram of the selected features: (**a**) stress range (blue), maximum stress (red), and static strength (green); (**b**) maximum stress-to-static strength ratio (purple), diameter (orange), and height (dark cyan); (**c**) height-to-diameter ratio (brown), compressive strength (pink), and ultimate strength (gray); (**d**) maximum stress-to-ultimate strength ratio (olive), elastic modulus of concrete (navy), and ratio of the elastic modulus of steel and concrete (magenta).

2.3.2. Pearson Correlation Coefficient Analysis

Pearson correlation coefficient analysis was conducted to evaluate the linearity between fatigue life and the previously selected features, ultimately selecting the most appropriate features for the machine learning models. The relationship between each feature and fatigue life revealed that the stress range, used in existing design codes, exhibited a strong negative correlation with fatigue life, with a coefficient of −0.83. In addition, the maximum stress-to-static strength ratio and maximum stress-to-ultimate strength ratio demonstrated a significant negative correlation of −0.5. This indicates that the failure modes defined during the feature engineering process were well reflected in the data. However, because both features involve the same variable (maximum stress), multicollinearity may occur in regression problems. Therefore, the maximum stress-to-static strength ratio and ultimate strength were selected as the final features. Finally, diameter and height also exhibited a negative correlation, of approximately −0.3, with fatigue life (Figure 6).

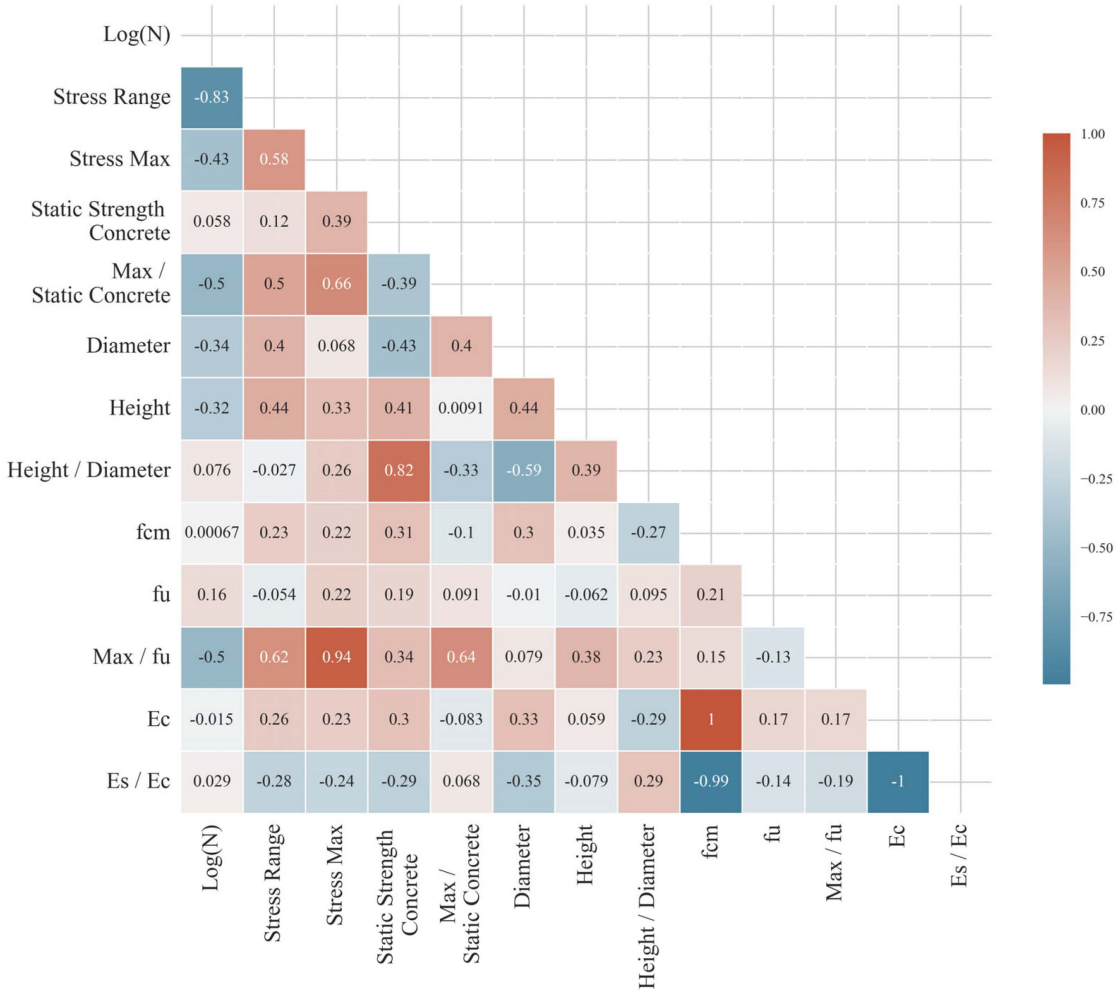


Figure 6. Pearson correlation coefficient analysis of the selected features.

2.4. Dataset for Fatigue Life Prediction

The final dataset for fatigue life prediction comprised of the following features: stress range, maximum stress-to-static strength ratio, ultimate strength, diameter and height, as listed in Table 3.

Table 3. Dataset for fatigue life prediction.

Input Feature	Mean	Min.	Max.	Std.	Unit
Stress range	120.798390	30.000000	179.270000	35.338377	MPa
Max stress/static strength	0.323189	0.059405	0.610717	0.097370	None
Ultimate strength	441.546752	337.855000	527.881200	39.703144	MPa
Diameter of stud	21.710124	10.000000	31.750000	5.602554	mm
Height of stud	117.742759	74.900000	155.000000	23.579766	mm
Output Feature	**Mean**	**Min.**	**Max.**	**Std.**	**Unit**
Log(N)	5.628602	3.725912	7.496943	0.816981	Cycle

3. Mahine Learning Models

3.1. Model Selection

3.1.1. AutoML Process

Based on the final data set defined in this study, various machine learning models were analyzed and compared to predict the fatigue life of headed studs using AutoML-based Pycaret [32] in Python and MATLAB Regression Learner [33]. The MATLAB Regression Learner automates the training, validation, and testing processes of the regression models. It allows for comparison across various regression models, including tree-based models and Bayesian-based models, such as Gaussian Process Regression (GPR) models. Pycaret, an open-source, low-code machine learning library in Python, automates the entire machine learning workflow from preprocessing to hyper parameter tuning and model evaluation. Pycaret leverages a wide range of modern machine learning models, such as XGBoost [34], CatBoost [35] and those from scikit-learn [36], providing a comprehensive comparison of the results across multiple models.

3.1.2. Metrics for Model Performance Evaluation

Four metrics were used to evaluate the performance of various models. The mean absolute error (MAE) is the average of the absolute differences between the predicted and actual values. The MAE provides a straightforward measure of error because it quantifies errors without considering their directions. This metric is robust against outliers, because it does not penalize large deviations. However, it may offer a conservative assessment of models when significant deviations occur.

$$MAE = \frac{1}{n}\sum_{i=1}^{n}|y_i - \hat{y}_i| \tag{8}$$

The mean squared error (MSE) is the average of the squared differences between the predicted and actual values. Unlike the MAE, the MSE squares the errors, assigning a larger penalty to larger errors, making it more sensitive to outliers. The square of errors has squared unites of the target variable. Therefore, the root mean squared error (RMSE), which is simply the square of the MSE, is also used for comparing model performances.

$$MSE = \frac{1}{n}\sum_{i=1}^{n}(y_i - \hat{y}_i)^2 \tag{9}$$

$$RMSE = \sqrt{\frac{1}{n}\sum_{i=1}^{n}(y_i - \hat{y}_i)^2} \tag{10}$$

R-squared is the coefficient of determination used to measure the proportion of variance in the target value that can be predicted from the independent variables. It is calculated as shown in Equation (11). R-squared ranges from 0 to 1, with higher values indicating that the model explains a larger proportion of the variance. This makes it a useful and intuitive

metric for comparing model performances. However, R-squared does not directly account for prediction errors. Therefore, it should be used in conjunction with other evaluation metrics for a more comprehensive assessment of model performance.

$$R^2 = 1 - \frac{\sum_{i=1}^{n}(y_i - \hat{y}_i)^2}{\sum_{i=1}^{n}(y_i - \overline{y})^2} \quad (11)$$

where

y_i = Actual value
$\hat{y}_i$ = Predicted value
$\hat{y}$ = Mean of actual values
n = Number of data

3.1.3. Model Selection

The performance metrics of various models were compared to select an appropriate machine learning model. The dataset was split into 80% training data and 20% test data, and cross-validation was performed using the K-fold method with five folds. To ensure balanced learning and numerical stability across various model types, all features were scaled to a range between 0 and 1 using a standard scaler. Machine learning models were categorized into tree-based models, ridge regressor, support vector machines, and Gaussian process regressions. Twelve individual models were evaluated based on different sub-models or hyperparameters, with their performance metrics for the test data are summarized in Table 4.

Table 4. Comparison of machine learning models.

Category	Model	MAE	MSE	RMSE	R-Squared
Tree-based model	Gradient boosting regressor	0.2596	0.1338	0.3591	0.7859
	AdaBoost regressor	0.3203	0.1722	0.4092	0.7278
	Light gradient boosting	0.3411	0.1870	0.4236	0.7115
	Extreme gradient boosting	0.3110	0.1848	0.4221	0.7039
	Random forest regressor	0.2992	0.1585	0.3919	0.7464
Ridge regressor	Ridge regression	0.3740	0.1988	0.4439	0.6861
	Kernel ridge regression	0.36947	0.21092	0.45926	0.73712
Support vector machine	Medium gaussian	0.34547	0.2027	0.45023	0.74736
	Quadratic	0.42196	0.27556	0.52494	0.65656
Gaussian process regression	Rational quadratic	0.32	0.15677	0.39594	0.80461
	Matern 5/2	0.32515	0.16166	0.40207	0.79851
	Squared exponential	0.32667	0.16615	0.40761	0.79292
	Exponential	0.29939	0.14345	0.37875	0.82121

Each metrics was calculated based on the test data.

Overall, the best-performing machine learning model was a Gaussian process regression, with the rational quadratic kernel achieving an MAE of 0.34, MSE of 0.15677, RMSE of 0.39594, and R-squared of 0.80461. The next best model was the gradient-boosting regressor (GBR), a tree-based model, achieving an MAE of 0.2596, MSE of 0.1338, RMSE 0.3591, and an R-Squared of 0.7859. Consequently, the GPR model was selected as the final model, and a fine-tuning process was conducted to optimize and further improve the prediction accuracy.

3.2. Fine-Tuning Models

The models and model parameters that were fine-tuned for the GBR and GPR, selected through an earlier model selection process, are as follows.

3.2.1. Gradient-Boosting Regressor (GBR)

Boosting algorithms aim to "boost" the small advantage that a hypothesis produced by a weak learner can achieve over random guessing, by repeatedly applying the weak learning procedure on a sequence of carefully constructed distributions [37]. The GBR is a boosting algorithm that combines decision trees to effectively model nonlinear relationships. Each tree model is sequentially trained with subsequent models to reduce the residual errors of previous models. During the training process new models are added to minimize residuals within each tree, and the final prediction is derived by aggregating the weighted outputs of all tree models. In this process the predictions are adjusted by following the gradient of the loss function from the objective function and fitting new models to the residual errors. This approach results in a model with high predictive performance.

The random grid search method was used to fine-tune the GBR. Table 5 summarizes the optimized model parameters obtained through this fine-tuning process.

Table 5. Hyperparameters of gradient-boosting regressor (GBR).

Model	Parameter	Value
Gradient boosting regressor	Loss	squared_error
	Learning rate	0.4
	N estimators	200
	Subsample	0.9
	Criterion	Friedman_mse
	Min. sample split	9
	Min. sample leafs	3
	Max. depth	1
	Min. impurity decrease	0.05
	Max. features	1.0
	Alpha	0.9
	Tol	10^{-4}
	Ccp alpha	0.0
	Max. features	1.0

3.2.2. Gaussian Process Regression (GPR)

GPR is a probabilistic supervised machine learning method that assumes the data follow a Gaussian distribution. The model is defined for all pairs of data points using a covariance function (kernel function), that reflects prior knowledge and measures the similarity between data points. This kernel function enables the prediction of new data and provides uncertainty quantification for these predictions. The parameters of the GPR model were optimized using the limited-memory Broyden–Fletcher–Goldfarb–Shanno-bound (L-BFGS-B) algorithm. Table 6 lists the optimized model parameters.

Table 6. Hyperparameters of Gaussian process regression (GPR).

Model	Parameter	Value
Gaussian process regression	Kernel	Constant × Rational Quadratic + White Kernel
	Alpha	10^{-10}
	Optimizer	fmin_l_bfgs_b
	N restart optimizer	50
	Normalize y	True
	Constant value	1.0
	Constant value bounds	0.001, 1000
	Kernel length scale	1.0
	Kernel length scale bounds	0.001, 1000
	Kernel alpha	0.1
	Kernel alpha bounds	10^{-10}, 1000.0
	Noise level	1.0

4. Results and Discussion

4.1. Prediction Accuracy of Machine Learning Models

Figure 7 compares the performances of the two proposed machine learning models in predicting stress range based on the test data. The fine-tuned GBR achieved an RMSE of 0.336 and R-squared value of 0.844 for the test data. The GPR model achieved an RMSE of 0.277 and R-squared value of 0.862. Both models demonstrated high accuracy in the training and testing phases, indicating that they were well-generalized and effectively predicted the fatigue life of shear studs on new data.

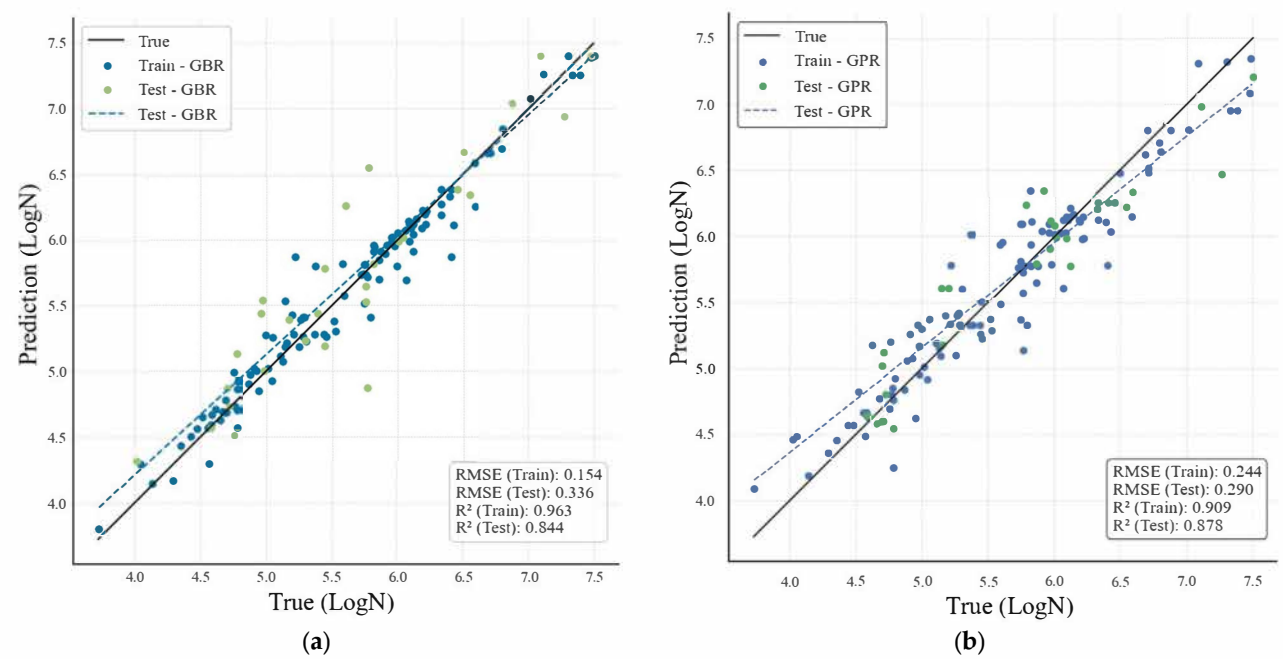


Figure 7. Comparison of model accuracy between machine learning models: (**a**) gradient-boosting regressor; (**b**) Gaussian process regression.

Figure 8 compares the predictions of existing design codes and those of the GPR model with respect to the stress range. The comparison was conducted under the same conditions with the parameters set to $d = 22$ mm, $h = 150$ mm, $f_u = 500$ MPa, $f_c = 35$ MPa. For the GPR model, the maximum stress to static strength ratio was fixed at 0.3, close to the dataset average. The results in Figure 8 indicate that the design codes, based on past experimental data, tend to be more conservative in their fatigue life predictions across the stress range compared with the proposed model. However, when uncertainty for the GPR model was quantified using a 95% confidence interval (CI), a higher level of uncertainty was observed at lower stress ranges. This increased uncertainty was attributed to the limited data available at a lower stress range and the presence of run-out data when fatigue failure did not occur. This uncertainty and prediction are expected to improve as the model is further trained using additional experimental data, enhancing the robustness and reliability of the predictions.

Figure 9 illustrates the accuracy and the distribution of the residual error from test dataset for the GPR model and its 95% CI, as well as for the AASHTO and Eurocode models. The figure shows that the AASHTO model demonstrates a conservative design approach, significantly underestimating fatigue life compared with the actual data. Specifically, the AASHTO model exhibits a high RMSE of 3.224, which is 8.4 times higher than the GPR model's RMSE of 0.384. By contrast, the Eurocode model provided predictions closer to the test data but tended to overestimate fatigue life at lower stress ranges, resulting in an RMSE of 0.878, which is still more than twice as high as RMSE of the GPR model. In addition, the GPR model and its 95% CI exhibited greater predictive accuracy than existing design codes by effectively training on the dataset. And the residual errors of the GPR model and

its 95% CI were evenly distributed, indicating a low prediction bias in both models when compared with the test data.

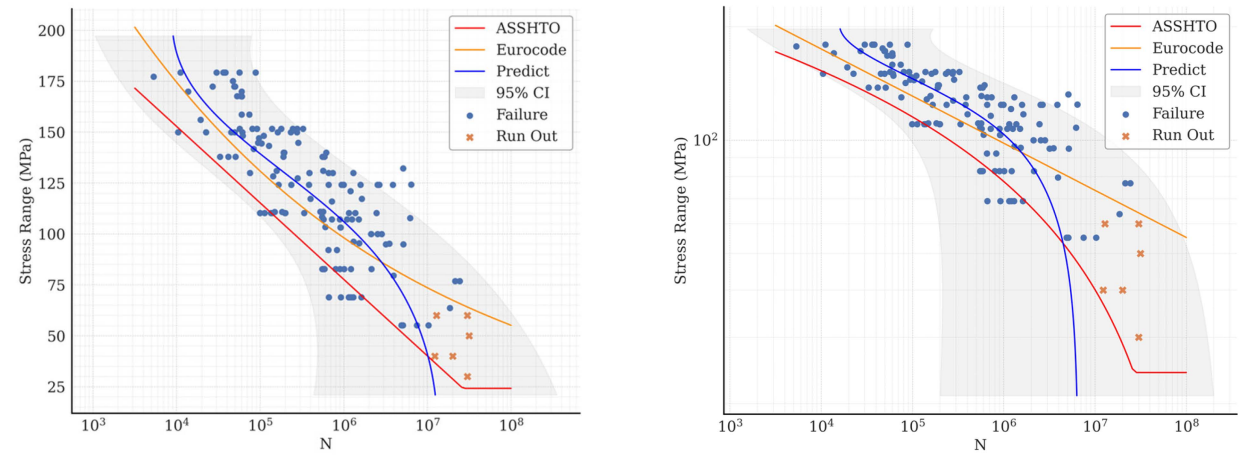


Figure 8. Comparison between machine learning models and existing design codes by stress range with $d = 22$ mm, $h = 150$ mm, $f_u = 450$ MPa, $f_c = 35$ MPa, and $\sigma_{max}/Q_{u,concrete} = 0.3$: (**a**) semi log scale; (**b**) log scale on stress range.

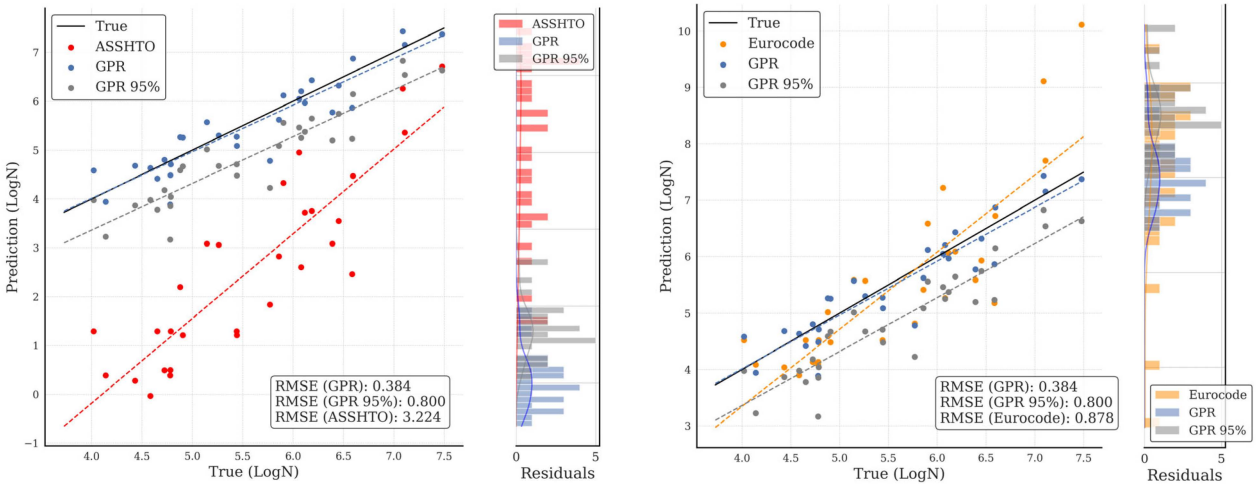


Figure 9. Comparison of model accuracy and residual errors between machine learning models and current design codes: (**a**) GPR and ASSHTO; (**b**) GPR and Eurocode.

Therefore, the proposed GPR model for predicting fatigue life provided reliable predictions with high accuracy and generalization performance and effectively accounting for the uncertainty by considering features previously overlooked by existing design codes.

4.2. Feature Importance Analysis

4.2.1. Individual Conditional Expectation (ICE)

The proposed machine learning models demonstrated high accuracy in predicting fatigue life, both the training data and on new data from test datasets. However, unlike simple empirical formulas, many machine learning models are complex, multidimensional regression models, which can be difficult for engineers to interpret, limiting their applicability in for decision-making. Therefore, this study used ICE [38] and SHAP [39] values to examine how the predicted fatigue life changes with variations in each selected feature and analyze feature importance.

ICE is a visualization technique that shows how the target value changes at individual data points for each feature. An ICE plot illustrates how the model's predictions vary with changes in a specific input variable, allowing the assessment of the sensitivity of the model to that input variable. For each feature, the predicted changes for the individual data points in the existing dataset are represented by individual lines. In addition, the plot includes lines representing the mean, as well as the 5th and 95th percentiles, to analyze the overall trend of each feature while excluding excessive variations or noise.

Figure 10, the ICE plot used to understand the relationship between each feature and fatigue life in proposed machine learning model, was analyzed according to the range of the dataset as specified in Table 3. For the stress range, a strong negative linearity with fatigue life was observed within the range of 35 MPa to 180 MPa, with a relatively uniform data distribution resulting in lower uncertainty compared with other features. The maximum stress to static strength ratio exhibited an overall negative linearity within the range of 0.05 to 0.6. This indicates that the maximum stress of each stud by cyclic load tend to reduce fatigue life. By contrast, the concrete static strength tended to increase fatigue life, as reflected by the model. The ultimate strength of the stud generally exhibited a positive correlation, particularly for using high-strength studs above 450 MPa. Indicating significant impact on fatigue life. For diameter and height, a slightly nonlinear relationship was observed within the ranges of 10 mm to 30 mm, and 60 mm to 160 mm, respectively. However, owing to the limited number of large-diameter stud experiments within the collected data, higher uncertainty was observed. This indicates that need for additional experimental data on various diameters to improve the reliability of the model.

4.2.2. SHapley Addictive exPlanations (SHAP) Value

SHAP calculates the contribution of each feature to the prediction, providing an overall understanding of the extent to which the model relies on each feature. While ICE visualizes the trend for each data point, SHAP shows how the relative value of each feature contributes to the prediction, allowing for the assessment of the overall feature importance based on mean SHAP values. Figure 11 shows the SHAP values and their averages for the GBR and GPR models. Both models identified stress range as the most significant feature, particularly in higher stress ranges (represented by red data points), where it demonstrated a substantial negative impact on the predicted values.

For the GBR, the next most influential features were, height, maximum stress to static strength ratio, ultimate strength, and diameter. By contrast, the GPR model identified the maximum stress to static strength ratio, ultimate strength, height, and diameter, as most important features following the stress range. In both models, stress range is considered the most important feature. However, in the GBR model, the effect of stress range is observed across a wider range (-1.5 to 1.5), whereas in the GPR model, it constrained to a smaller range (-1.0 to 1.0). This suggests that the influence of Stress Range is relatively lower in the GPR model compared to the GBR model, allowing other features to be considered more significant in the GPR model. In addition, while the GBR model considers height, which exhibits a relatively discrete distribution, as a key feature, the GPR model identifies the maximum stress to static strength ratio as the next most important variable, with a more evenly distributed SHAP value. Moreover, the GBR model as the interactions between features based on tree structure with a structural and hierarchical method, leading to more discontinuous patterns in SHAP values compared to the GPR model. As a result, the GPR model displayed relatively more distinct feature importance than the GBR model.

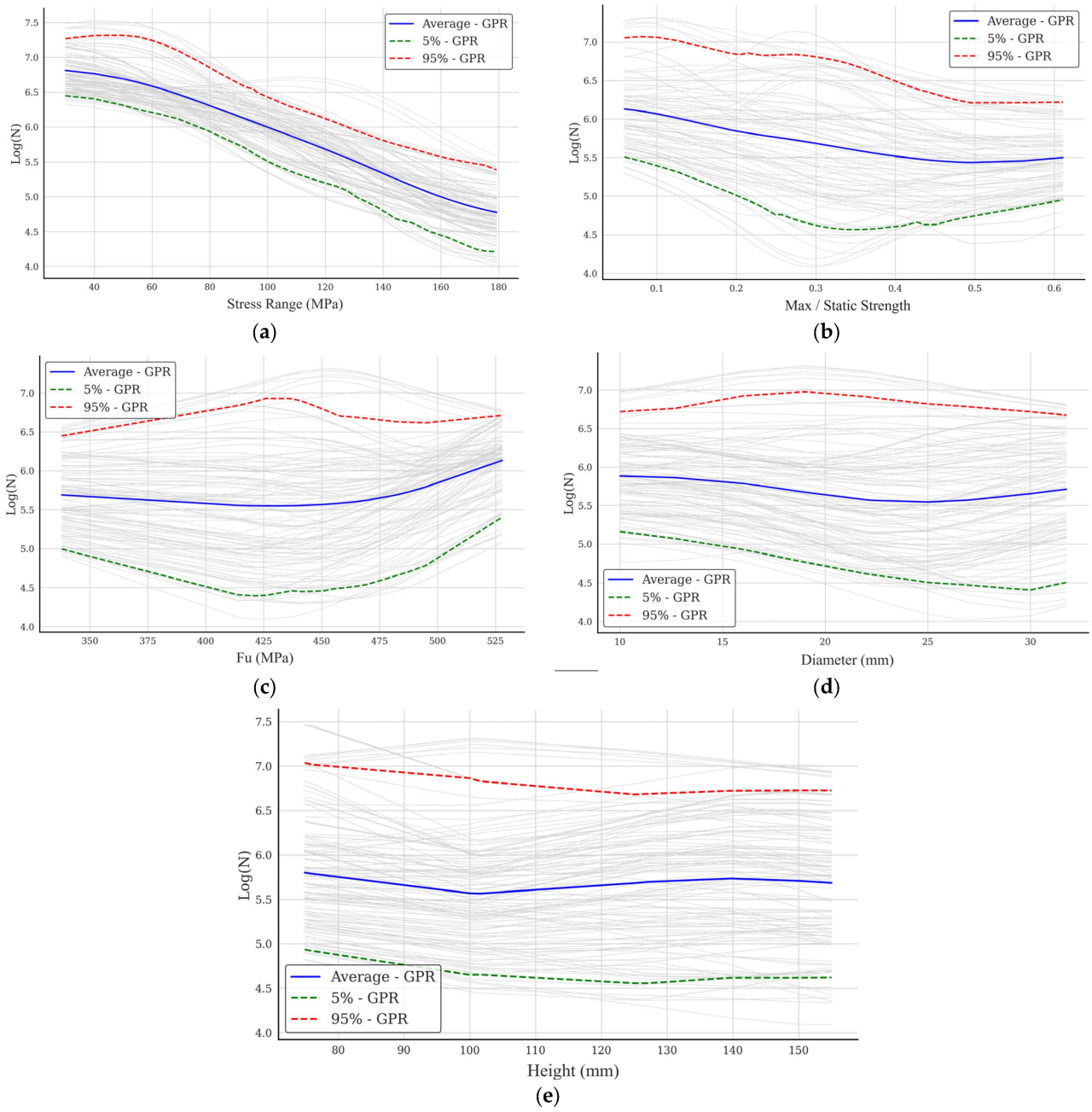


Figure 10. Individual conditional expectation (ICE) plot of Gaussian process regression: (**a**) stress range; (**b**) max./static strength; (**c**) ultimate strength; (**d**) diameter; (**e**) height.

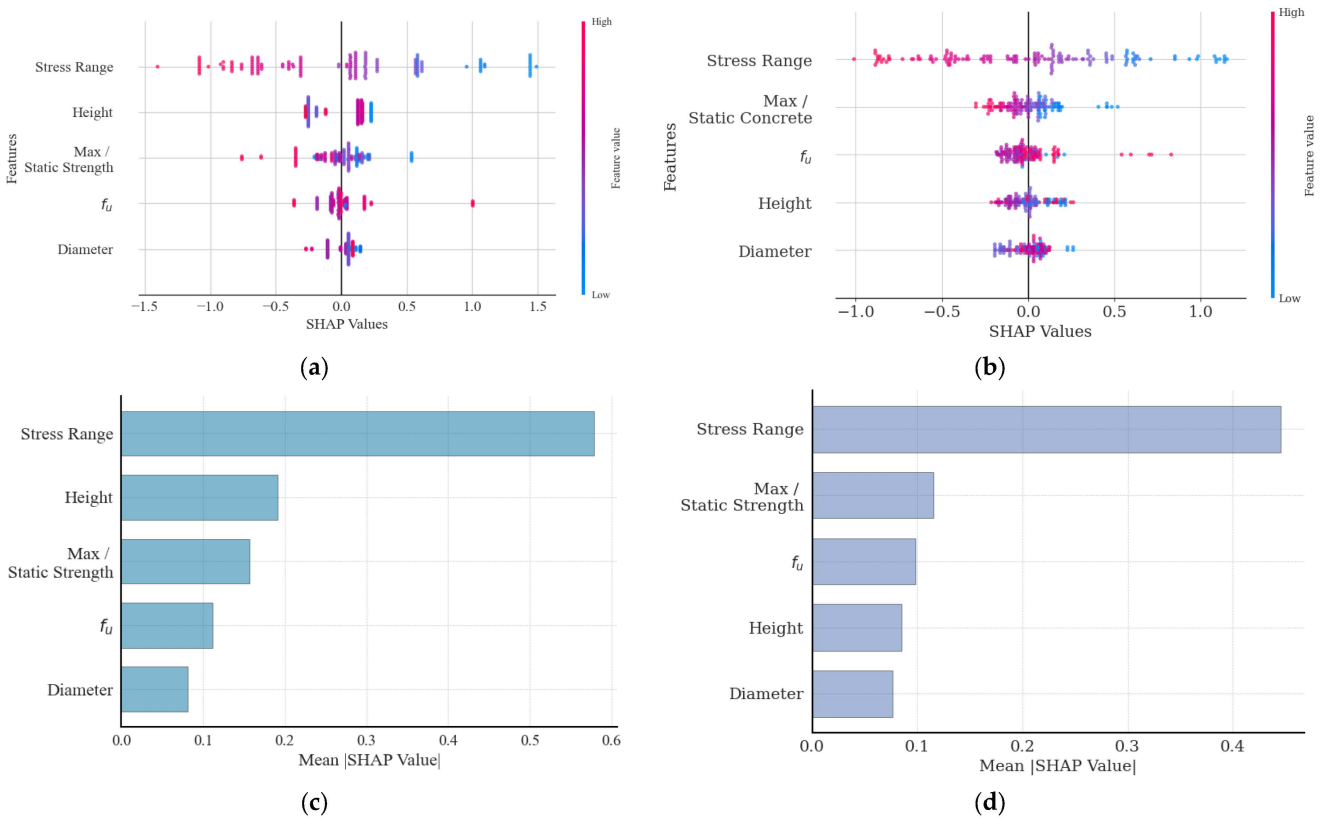


Figure 11. Comparison of SHAP values between machine learning models and current design codes: (**a**) SHAP values of GBR; (**b**) SHAP value of GPR; (**c**) mean SHAP values of GBR; (**d**) mean SHAP values of GPR.

5. Conclusions

Current methods for predicting fatigue life in existing design codes heavily rely on historical experimental data. However, these methods often fail to address the diverse conditions encountered in actual steel concrete composite bridges, such as the use of high-strength materials and precast decks. In addition, the inherent eccentricity in single-sided push-out tests increases crack propagation, leading to overly conservative fatigue life predictions in design codes. Furthermore, the conventional employed statistical technique, the least-squares regression approach, fails to adequately account for uncertainties in confidence levels. This limitation reduces the generalization performance and complicates the assessment of the reliability of predictive outcomes.

To overcome the limitations of existing design codes, this study proposed a machine learning model for predicting the fatigue life of stud shear connectors. The model employs feature engineering to capture critical aspects of fatigue behavior and uses feature selection to evaluate the linearity between variables. The model aims to significantly improve the accuracy of fatigue life predictions by identifying the key factors contributing to fatigue failure and leveraging a comprehensive dataset of push-out test results. The performance and uncertainty of the proposed model were rigorously validated by comparing its predictions with those of existing design codes, using test data excluded from the training phase.

In addition, the impact of each selected feature of fatigue life was analyzed through ICE plots, illustrating the localized relationship between the fatigue life and each feature, as well as SHAP values, which assess the overall trends and feature importances.

The following conclusions were drawn from this process:

1. Through the feature engineering process, the overall fatigue behavior was categorized into four factors: shear transfer, crack initiation, crack propagation, and failure. Twelve features based on these four factors were selected. Based on their linearity with fatigue

life, key features such as stress range, maximum stress-to-static strength ratio, ultimate strength, diameter, and height were identified. These key features were applied to a dataset of approximately 146 push-out tests.

2. To select the most appropriate machine learning model for predicting fatigue life, 12 different models were compared using Pycaret and MATLAB AutoML Process. The GPR model was identified as the most appropriate model exhibiting the highest performance metrics. This model, along with its associated uncertainties, was compared to existing design codes using test data to, analyzing the prediction accuracy and the distribution of residual errors. The results demonstrated that the proposed GPR model provided reliable predictions with high accuracy and generalization performance while effectively accounting for uncertainty by incorporating features previously overlooked in existing design codes.
3. Feature importance analysis based on the proposed GPR model revealed that the stress range most significantly influenced fatigue life prediction. The maximum stress-to-static strength ratio and ultimate strength also exhibited a significant influence. Although the diameter and height, related to stud geometry, exhibited relatively lower importance, they affected fatigue life prediction through certain nonlinear relationships. In addition, the prediction results of the proposed GPR model, along with the feature importance analysis, indicate that each feature exhibits high uncertainty when predicting outside the dataset range specified in Table 3. Therefore, it is recommended to make predictions within this range, and these restrictions can be mitigated with the acquisition of additional data in the future.
4. For the further study, the proposed model, which can replace the empirical equations in existing design codes, can be used as follows: a pretrained model is developed using global data, which includes experimental results sourced from the literature. These data are preprocessed, and the machine learning model is trained to generalize across diverse conditions. Once the pretrained model is established, the second step involves fine-tuning the model using local data specific to the country of interest. Local experimental data, reflective of regional conditions such as materials and practices, are used to adjust the parameter of pretrained model, ensuring accurate representation of the local situation. The fine-tuned model is then integrated into local design codes, replacing empirical equations with a data-driven approach. Continuous validation and monitoring are essential to ensure reliability of the model in practical applications.

Author Contributions: Conceptualization, C.-S.S.; methodology, D.-H.K.; validation, D.-H.K.; investigation, D.-H.K.; resources, D.-H.K., C.-S.S. and K.-C.L.; data curation, D.-H.K. and G.-T.R.; writing—original draft preparation, D.-H.K.; writing—review and editing, C.-S.S., K.-C.L. and G.-T.R.; visualization, D.-H.K.; supervision, C.-S.S.; project administration, C.-S.S.; funding acquisition, C.-S.S. All authors have read and agreed to the published version of the manuscript.

Funding: This research was conducted with the support of the "National R&D Project for Smart Construction Technology (RS-2020-KA156007)", funded by the Korea Agency for Infrastructure Technology Advancement under the Ministry of Land, Infrastructure and Transport, and managed by the Korea Expressway Corporation. Moreover, this research was supported by the Chung-Ang University Research Scholarship Grants in 2023.

Data Availability Statement: The data presented in this study are available at https://github.com/easternwise98/fatigue-life-prediction.git (accessed on 8 October 2024).

Conflicts of Interest: The authors declare no conflicts of interest.

References

1. Slutter, R.G.; Fisher, J.W. Fatigue Strength of Shear Connectors. *Highw. Res. Rec.* **1966**, *147*, 65–88.
2. AASHTO American Association of State Highway and Transportation Officials. *LRFD Bridge Design Specifications*, 9th ed.; AASHTO American Association of State Highway and Transportation Officials: Washington, DC, USA, 2020.
3. Oehlers, D.; Foley, L. The Fatigue Strength of Stud Shear Connections in Composite Beams. *Proc. Inst. Civ. Eng.* **1985**, *79*, 349–364. [CrossRef]

4. Johnson, R.P. Resistance of Stud Shear Connectors to Fatigue. *J. Constr. Steel Res.* **2000**, *56*, 101–116. [CrossRef]
5. *1994-2 Eurocode 4*; Design of Composite Steel and Concrete Structures, General Rules and Rules for Bridges. European Commission: Brussels, Belgium, 2005.
6. Hanswille, G.; Porsch, M.; Ustundag, C. Resistance of Headed Studs Subjected to Fatigue Loading. *J. Constr. Steel Res.* **2007**, *63*, 475–484. [CrossRef]
7. Hanswille, G.; Porsch, M.; Ustundag, C. Resistance of Headed Studs Subjected to Fatigue Loading Part II: Analytical Study. *J. Constr. Steel Res.* **2007**, *63*, 485–493. [CrossRef]
8. Badie, S.S.; Tadros, M.K.; Kakish, H.F.; Splittgerber, D.L.; Baishya, M.C. Large Shear Studs for Composite Action in Steel Bridge Girders. *J. Bridge Eng.* **2002**, *7*, 195–203. [CrossRef]
9. Lee, P.-G.; Shim, C.-S.; Chang, S.-P. Static and Fatigue Behavior of Large Stud Shear Connectors for Steel–Concrete Composite Bridges. *J. Constr. Steel Res.* **2005**, *61*, 1270–1285. [CrossRef]
10. Liu, Y.; Zhang, Q.; Bao, Y.; Bu, Y. Static and Fatigue Push-out Tests of Short Headed Shear Studs Embedded in Engineered Cementitious Composites (ECC). *Eng. Struct.* **2019**, *182*, 29–38. [CrossRef]
11. Shim, C.-S.; Lee, P.-G.; Chang, S.-P. Design of Shear Connection in Composite Steel and Concrete Bridges with Precast Decks. *J. Constr. Steel Res.* **2001**, *57*, 203–219. [CrossRef]
12. Shim, C.-S.; Lee, P.-G.; Kim, D.-W.; Chung, C.-H. Effects of Group Arrangement on the Ultimate Strength of Stud Shear Connection. In *Composite Construction in Steel and Concrete VI*; American Society of Civil Engineers: Tabernash, CO, USA, 2011; pp. 92–101.
13. Okada, J.; Yoda, T.; Lebet, J.-P. A study of the grouped arrangements of stud connectors on shear strength behavior. *Struct. Eng. Earthq. Eng.* **2006**, *23*, 75s–89s. [CrossRef]
14. Shim, C.-S.; Kim, D.-W. Structural Performance of Composite Joints Using Bent Studs. *Int. J. Steel Struct.* **2010**, *10*, 1–13. [CrossRef]
15. Lee, K.-C.; Abbas, H.H.; Ramey, G.E. Review of Current AASHTO Fatigue Design Specifications for Stud Shear Connectors. In *Structures Congress 2010*; American Society of Civil Engineers: Orlando, FL, USA, 2010; pp. 310–321.
16. Avci-Karatas, C. Application of Machine Learning in Prediction of Shear Capacity of Headed Steel Studs in Steel–Concrete Composite Structures. *Int. J. Steel Struct.* **2022**, *22*, 539–556. [CrossRef]
17. Roh, G.-T.; Vu, N.; Jeon, C.-H.; Shim, C.-S. Augmented Data-Driven Machine Learning for Digital Twin of Stud Shear Connections. *Buildings* **2024**, *14*, 328. [CrossRef]
18. Roshanfar, M.; Ghiami Azad, A.R.; Forouzanfar, M. Predicting Fatigue Life of Shear Connectors in Steel-concrete Composite Bridges Using Artificial Intelligence Techniques. *Fatigue Fract. Eng. Mater. Struct.* **2024**, *47*, 818–832. [CrossRef]
19. Oehlers, D.J.; Bradford, M.A. *Composite Steel and Concrete Structural Members: Fundamental Behaviour*, 1st ed.; Pergamon: Oxford, UK; Tarrytown, NY, USA, 1995; ISBN 978-0-08-041919-0.
20. Bro, M.; Westberg, M. Influence of Fatigue on Headed Stud Connectors in Composite Bridges. Master's Thesis, Luleå Tekniska Universitet, Luleå, Sweden, 2004.
21. Paris, P.; Erdogan, F. A Critical Analysis of Crack Propagation Laws. *J. Basic Eng.* **1963**, *85*, 528–533. [CrossRef]
22. Mainstone, R.J.; Menzies, J.B. Shear connectors in steel-concrete composite beams for bridges. I. static and fatigue tests on push-out specimens. *Concrete* **1967**, *1*, 291.
23. National Research Council (U.S.), Highway Research Board. *Highway Research Record*; National Research Council, Highway Research Board: Washington, DC, USA, 1968.
24. Oehlers, D.J. Deterioration in Strength of Stud Connectors in Composite Bridge Beams. *J. Struct. Eng.* **1990**, *116*, 3417–3431. [CrossRef]
25. Zandonini, R.; Bursi, O.S. Cyclic Behavior of Headed Stud Shear Connectors. In *Composite Construction in Steel and Concrete IV*; American Society of Civil Engineers: Banff, AB, Canada, 2002; pp. 470–482.
26. Feldmann, M.; Hechler, O.; Hegger, J.; Rauscher, S. Fatigue Behavior of Shear Connectors in High Performance Concrete. In *Composite Construction in Steel and Concrete VI*; American Society of Civil Engineers: Tabernash, CO, USA, 2011; pp. 39–51.
27. Mundie, D.L. Fatigue Testing and Design of Large Diameter Shear Studs Used in Highway Bridges. Master's Thesis, Auburn University, Auburn, AL, USA, 2011.
28. Xie, E.; Valente, M.I.B. *Research Report Fatigue Strength of Shear Connectors*; University of Minho: Guimarães, Portugal, 2011.
29. Dogan, O.; Roberts, T.M. Fatigue Performance and Stiffness Variation of Stud Connectors in Steel–Concrete–Steel Sandwich Systems. *J. Constr. Steel Res.* **2012**, *70*, 86–92. [CrossRef]
30. Ovuoba, B.; Prinz, G.S. Fatigue Capacity of Headed Shear Studs in Composite Bridge Girders. *J. Bridge Eng.* **2016**, *21*, 04016094. [CrossRef]
31. Wang, W.; Chen, J.; Jin, W. Experimental Investigation of Corroded Stud Shear Connectors Subjected to Fatigue Loading. *J. Mater. Civ. Eng.* **2017**, *29*, 04016175. [CrossRef]
32. Ali, M. PyCaret: An Open-Source, Low-Code Machine Learning Library in Python. Version 3.4. Available online: https://github.com/pycaret/pycaret (accessed on 8 October 2024).
33. The MathWorks, Inc. Statistics and Machine Learning Toolbox Documentation. Available online: https://www.mathworks.com/help/stats/index.html (accessed on 19 August 2024).
34. Chen, T.; Guestrin, C. XGBoost: A Scalable Tree Boosting System. In Proceedings of the 22nd ACM SIGKDD International Conference on Knowledge Discovery and Data Mining, San Francisco, CA, USA, 13–17 August 2016; pp. 785–794.
35. Friedman, J.H. Greedy Function Approximation: A Gradient Boosting Machine. *Ann. Statist.* **2001**, *29*, 1189–1232. [CrossRef]

36. Pedregosa, F.; Varoquaux, G.; Gramfort, A.; Michel, V.; Thirion, B.; Grisel, O.; Blondel, M.; Prettenhofer, P.; Weiss, R.; Dubourg, V.; et al. Scikit-Learn: Machine Learning in Python. *J. Mach. Learn. Res.* **2011**, *12*, 2825–2830.
37. Zemel, R.S.; Pitassi, T. A Gradient-Based Boosting Algorithm for Regression Problems. In Proceedings of the 13th International Conference on Neural Information Processing Systems (NIPS 2000), Denver, CO, USA, 27 November–2 December 2000; MIT Press: Cambridge, MA, USA, 2000.
38. Goldstein, A.; Kapelner, A.; Bleich, J.; Pitkin, E. Peeking Inside the Black Box: Visualizing Statistical Learning with Plots of Individual Conditional Expectation. *J. Comput. Graph. Stat.* **2015**, *24*, 44–65. [CrossRef]
39. Lundberg, S.M.; Lee, S.-I. A Unified Approach to Interpreting Model Predictions. In Proceedings of the 31st International Conference on Neural Information Processing Systems, Long Beach, CA, USA, 4–9 December 2017; Curran Associates, Inc.: Red Hook, NY, USA, 2017.

Disclaimer/Publisher's Note: The statements, opinions and data contained in all publications are solely those of the individual author(s) and contributor(s) and not of MDPI and/or the editor(s). MDPI and/or the editor(s) disclaim responsibility for any injury to people or property resulting from any ideas, methods, instructions or products referred to in the content.